Organic & Biomolecular Chemistry

ROYAL SOCIETY OF CHEMISTRY

PAPER

View Article Online
View Journal | View Issue

Cite this: *Org. Biomol. Chem.*, 2024, **22**, 2877

Overview of alkyl quercetin lipophenol synthesis and its protective effect against carbonyl stress involved in neurodegeneration†

Léa Otaegui,‡[a,b] Jordan Lehoux,‡[b] Leo Martin,[b] Laurent Givalois,[a,c] Thierry Durand,[b] Catherine Desrumaux[a,d] and Céline Crauste*[b]

Oxidative stress and carbonyl stress resulting from the toxicity of small aldehydes are part of the detrimental mechanisms leading to neuronal cell loss involved in the progression of neurodegenerative diseases such as Alzheimer's disease. Polyunsaturated alkylated lipophenols represent a new class of hybrid molecules that combine the health benefits of anti-inflammatory omega-3 fatty acids with the anti-carbonyl and oxidative stress (anti-COS) properties of (poly)phenols in a single pharmacological entity. To investigate the therapeutic potential of quercetin-3-docosahexaenoic acid-7-isopropyl lipophenol in neurodegenerative diseases, three synthetic pathways using chemical or chemo-enzymatic strategies were developed to access milligram or gram scale quantities of this alkyl lipophenol. The protective effect of quercetin-3-DHA-7-*i*Pr against cytotoxic concentrations of acrolein (a carbonyl stressor) was assessed in human SHSY-5Y neuroblastoma cells to underscore its ability to alleviate harmful mechanisms associated with carbonyl stress in the context of neurodegenerative diseases.

Received 12th January 2024,
Accepted 12th March 2024

DOI: 10.1039/d4ob00066h

rsc.li/obc

Introduction

It is commonly accepted that oxidative stress (*i.e.*, an imbalance between the reactive oxygen species and the antioxidant system or defense of the body) can have detrimental effects on neural tissues and be part of the etiology of neurodegenerative pathologies including Alzheimer's disease (AD).[1,2] Oxidative stress (OS) is an early and persistent feature of AD that can be of genetic origin or amplified by environmental factors such as smoking, pollution, or exposure to toxic substances. A direct consequence of OS is the increase in lipid peroxidation, leading to the formation of various aldehydic by-products, including malondialdehyde (MDA), 4-hydroxy-2-nonenal (HNE), and acrolein. Acrolein, the most reactive among them, can also originate from exogenous sources as it is commonly present in the environment as a pollutant. Reactive electrophilic aldehydes are the cause of carbonyl stress toxicity, as they form cellular adducts with nucleophilic proteins, lipids, or nucleic acids, and impair their function. A significant increase in acrolein and other carbonyl stressors was observed in the brain of early Alzheimer's patients,[3] associated with toxicity in hippocampal neurons.[4] Due to their high neurotoxicity, reactive aldehydes have been identified as neurotoxic mediators of oxidative damage in the progression of AD.[5–7]

A deficiency in polyunsaturated fatty acids (PUFAs), a critical class of fatty acids essential for brain functions, has also been identified as a factor contributing to increased oxidative stress.[8] Docosahexaenoic acid (DHA, 22:6 n-3), the most prevalent omega-3 PUFA in neuronal membranes,[9] possesses significant free radical scavenging properties and provides protection against peroxidative damage to brain lipids. It also serves as a precursor for the biosynthesis of lipid mediators that regulate inflammatory responses.[10] DHA is weakly produced *de novo* and must be obtained from the diet. In humans, low plasmatic concentrations of DHA have been associated with impaired cognitive function, low hippocampal volumes, and increased amyloid deposition in the brain.[11,12] Reduced DHA concentrations have been reported in the brains of AD patients.[13] A number of epidemiological studies suggest that dietary DHA consumption is essential for brain development, learning ability and memory, and prevention of cognitive decline.[14] However, the success of oral DHA supplementation (a highly oxidizable derivative) depends on individual variability, including that of metabolism.[15] Recently, we showed

[a]*MMDN, Univ Montpellier, INSERM, EPHE, Montpellier, France*
[b]*IBMM, Univ Montpellier, CNRS, ENSCM, 34000 Montpellier, France. E-mail: celine.crauste@umontpellier.fr*
[c]*Laval University, Department of Neurosciences & Psychiatry, Quebec, Canada*
[d]*LIPSTIC LabEx, 21000 Dijon, France*

†Electronic supplementary information (ESI) available: Additional information: all ^{1}H and ^{13}C NMR spectra of pure compounds, ^{1}H NMR spectra and chemical structures of S1, S2, and S3 isolated as mixtures, Table S1, and Fig. S1 and S2. See DOI: https://doi.org/10.1039/d4ob00066h

‡These authors contributed equally to this work as first authors.

that intranasal administration of nanovectorized DHA reduces tau phosphorylation and restores cognitive functions in two murine models of AD.[16] These results pave the way for the development of a new approach for targeting the brain using DHA for the prevention or treatment of AD.

Currently, clinical trials of many drugs targeting AD may have failed because of the single target-based therapeutics (and also the high impenetrability of the blood–brain barrier). In this context, carbonyl and oxidative stresses (COS), in addition to disrupting DHA homeostasis, emerge as interesting targets to combat the progression of AD and serve as the starting point for the development of multi-target pharmacological molecules.

There is currently growing interest in the impact of dietary nutrients on reducing toxic mechanisms leading to the onset of cognitive disorders,[17,18] particularly, (poly)phenols,[19] well-known antioxidant compounds abundant in fruits and vegetables. Interestingly, depending on their chemical structure, they can also efficiently act as anti-carbonyl stress agents by directly or indirectly trapping reactive aldehydes.[20,21] However, the pharmacological development of (poly)phenol drugs often encounters issues related to their high metabolism and low bioavailability. We have previously developed hybrid pharmacological protective molecules called lipophenols, based on the conjugation of PUFAs and (poly)phenols, to overcome PUFA degradation due to oxidation, enhance the bioavailability of (poly)phenols, provide DHA, and target PUFA-rich tissues such as the retina.[22] In addition, this approach allows us to leverage the therapeutic characteristics offered by both components of lipophenols (*i.e.*, the (poly)phenol and the PUFA). Alkyl lipophenols of DHA were efficient in providing cellular protection against oxidative and carbonyl stresses involved in age-related macular degeneration (AMD) or genetic Stargardt dystrophy.[23–25] The importance of the alkyl (an isopropyl) and the omega-3 chain has been highlighted in cellular models. Such new lipophenolic derivatives were able to protect photoreceptor degeneration induced by light (80% of protection) in a murine model of genetic macular degeneration by IV and oral administration,[26,27] thus validating the proof of concept of the pre-clinical interest of those PUFA conjugates.

Considering the close relationship between the COS mechanisms involved in AMD and AD and the essential physiological role of DHA in both retinal and brain functions, alkyl lipophenols of DHA should be evaluated for their potential as pharmacological agents to reduce COS associated with AD. In the present study, we selected quercetin-3-DHA-7-*i*Pr (for quercetin-3-docosahexaenoate-7-isopropyl, Fig. 1), the most efficient anti-COS lipophenol described so far,[24] for further investigation to reduce carbonyl stress involved in AD (*in vitro* first and then using *in vivo* models in the future). To achieve this goal, new synthetic methodologies for obtaining gram-scale quantities of this alkyl-PUFA lipophenol of quercetin are needed. Indeed, we previously observed that once *in vitro* screening is validated, the challenge of upscaling the chemical synthesis strategy of lipophenol could impede effective pre-clinical studies involving gram-scale consumption for toxicity evaluation, pharmacokinetic aspects or formulation development. Therefore, new chemical strategies to access quercetin-3-DHA-7-*i*Pr have been developed and compared based on their reproducibility, scalability, the number of steps involved and their potential to contribute to greener chemistry. This work thus highlights the strengths and weaknesses of three new different synthesis strategies. While each pathway leads to the desired molecule, not all meet the criteria required for the *in vivo* assessment of a therapeutically relevant compound. In the second phase of our study, we shift our focus to the evaluation of the synthesized quercetin-3-DHA-7-*i*Pr in the context of AD.

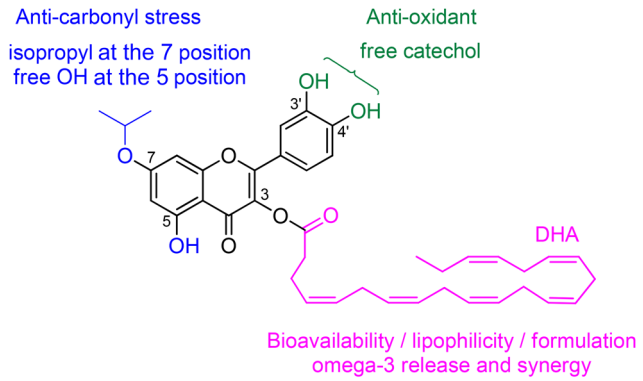

Fig. 1 Chemical structure of lipophenol quercetin-3-DHA-7-*i*Pr.

Using acrolein as a potent carbonyl stressor, we developed an efficient cellular assay to investigate the efficacy of this conjugate in protecting against carbonyl stress in human SH-SY5Y neuroblastoma cells. The potential of this conjugate to mitigate the toxic effects of acrolein and the importance of both the isopropyl and the PUFA part in its protective effect were evaluated.

Results and discussion

Chemical synthesis

Chemo-enzymatic pathway A. Close reactivity of phenolic functions of quercetin leads to mono, di and tri-acylated derivatives at positions 7, 3, 3′ and 4′ when acylation reactions are realized starting from unprotected quercetin.[28,29] Thus, the previously reported chemical synthesis of quercetin-3-DHA-7-*i*Pr was carried out in 9 steps using a strategy involving a protection/deprotection set of phenolic functions.[24] The use of 3 types of protecting groups for different OH functions (dioxole, triisopropylsilyl (TIPS) and acetate) was necessary to achieve the incorporation of the alkyl group only at the 7 position and the DHA at the specific 3 position. However, this strategy was reproducible only on the mg scale. In the perspective of modifying the synthesis strategy in line with the principles of sustainable chemistry (atom economy, less toxic chemical reagents, and use of green catalysts), the use of supported and

reusable enzymatic systems was considered to replace the protection/deprotection steps. Several lipases have been used to regioselectively acylate phenolic functions of stilbenoid or flavonoid polyphenols.[30–33] However, none of them were effective at selectively acylating and discriminating the different OH positions of the quercetin skeleton.[31] Moreover, the efficiency of the lipase is usually dependent on the carbon length of the fatty acid chain and the number of unsaturation, making the enzymatic incorporation of polyunsaturated fatty acids a real chemo-enzymatic challenge. We previously validated the use of the lipase Lipozyme® (supported lipase from *Mucor miehei*) as a powerful tool to synthesize the quercetin-3-DHA lipophenolic conjuguate.[34] Starting from penta-acylated quercetin, having DHA at positions 3′, 4′, 3, 5 and 7, the supported lipase was able to regioselectively deacylate all the phenolic positions, without affecting DHA ester at the third position. This reaction was reproducible on a gram scale in acceptable yield (unpublished data). Based on this observation, the synthesis of quercetin-3-DHA-7-*i*Pr was planned using a dioxole protecting group of the catechol function and benzyl protection for the phenolic function at the 3 position to allow alkyl incorporation only at the 7 position (Scheme 1). The incorporation of DHA could be performed after the completion of PUFA acylation and regioselective deacylation, thus reducing the initially described strategy by three steps. Starting from commercially available anhydrous quercetin (**1**), the catechol function was protected in the presence of dichlorodiphenylmethane in diphenyl ether as previously described.[24]

Then, the monobenzylation of the most reactive OH-3 function of compound **2** was carried out using carefully selected equivalents of benzyl bromide (to consume all of the starting compound **2** and avoid high proportion of di-benzylated **3b** –

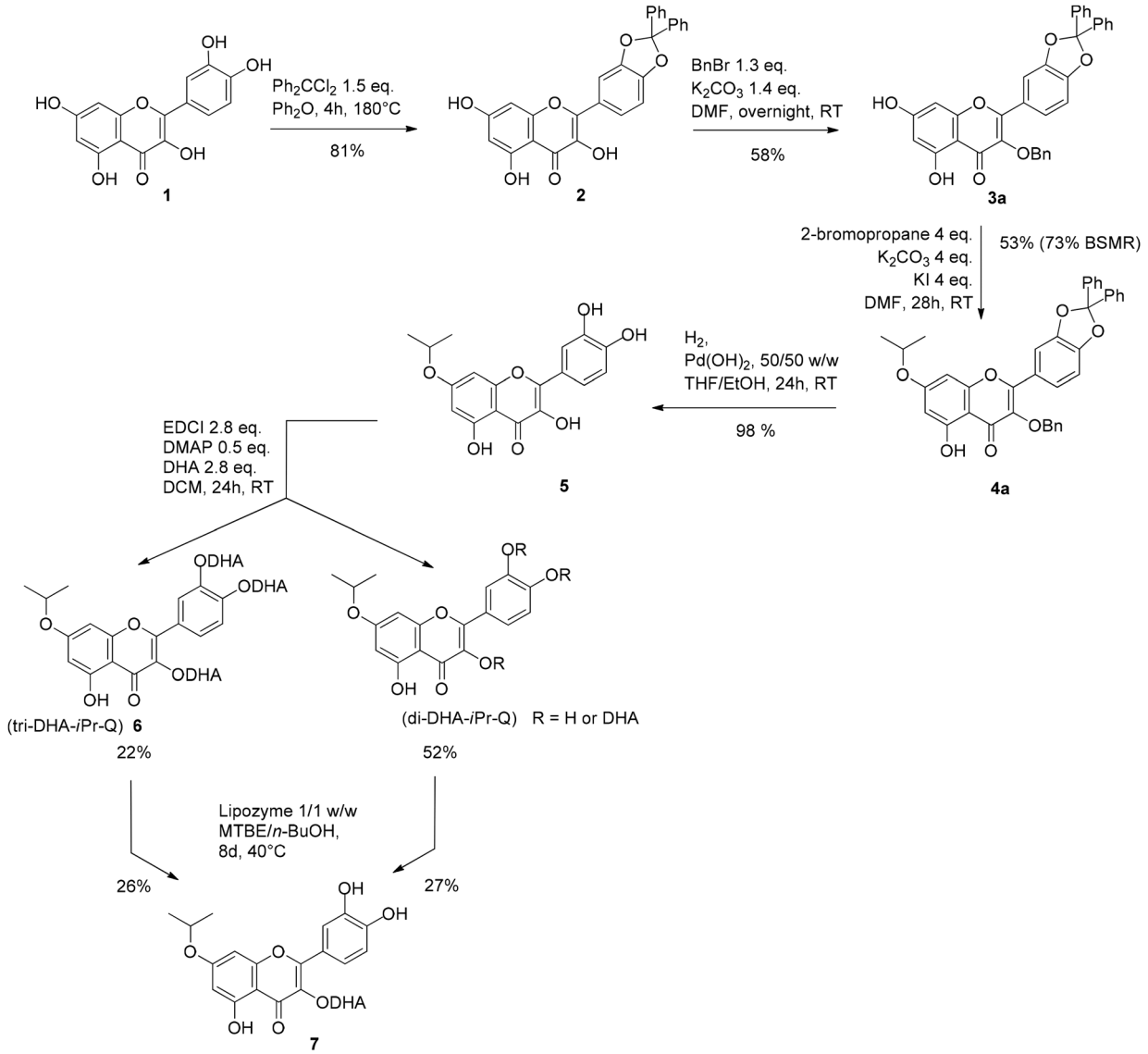

Scheme 1 Pathways A – chemo-enzymatic synthesis of quercetin-3-DHA-7-*i*Pr.

Table 1 Comparison of pathways **A**, **B1** and **B2**

Pathways	Nbr of steps	Global yield	Reproducibility of the strategy tested	Amount of compound 7 synthesized: each step performed once[a]	Amount of compound 7 synthesized: with batch reproduction
A "chemo-enzymatic"	7	4.6%	No	49 mg	nd
B1 "butyrate"	10	10.2%	No	630 mg	nd
B2 "acetate"	8	14.6%	Yes	994 mg	2.91 g

[a] On scale tested, starting from 5 g of quercetin.

Table S1†).[35] The selective alkylation at the 7 position of **3a** was performed as the one described for the total synthesis of rhamnetin, the 7-methyl analogue of quercetin.[35] The well-known hydrogen bonding between the OH-5 and the carbonyl function reduces the activity at the 5 position, allowing for regioselective alkylation at the 7 position. In contrast to methylation, isopropylation requires a greater amount of reagent to achieve an efficient conversion in mono-isopropylated **4a**, due to a lower reactivity of the sterically hindered iodopropane. When one manages to limit dialkylation (**4b**), the remaining starting material can be easily recovered resulting in an acceptable 53% yield (73% BSMR). Hydrogenation of **4a** was then performed using palladium hydroxide under hydrogen to achieve both deprotection of dioxole and benzyl protecting groups with excellent yields. Based on preliminary work (see Fig. S1†), the coupling reaction with DHA was then conducted to minimize the introduction of the fatty acid at the 5 position. Indeed, this position is poorly hydrolysable by the enzyme in the presence of an isopropylated bulky group located at the 7 position. Tri-DHA quercetin **6** was thus isolated in moderate yield (22%) and the absence of DHA at the 5 position was confirmed by the unshielded characteristic ^{1}H NMR signal of the OH-5 position at 12.05 ppm (Scheme 1). A mixture of di-DHA derivatives (uncharacterized) was also obtained (52%) and used as tri-DHA **6** in regioselective enzymatic deacylation. Due to the long C22 carbon chain and the presence of six unsaturated bonds, DHA is not enzymatically cleaved as quickly as a shorter, saturated fatty acid.[32] The reaction reaches a plateau after 6–8 days, and neither the addition nor the replacement of the supported lipase improves the final yield. The desired quercetin-3-DHA-7-*i*Pr (**7**) was recovered using either a tri-DHA (**6**) or di-DHA mixture. Overall, we have successfully developed a new methodology, leveraging the regioselectivity of the Lipozyme® lipase, to access an alkyl lipophenol of quercetin with a reduced number of steps (Table 1). It is worth noting that this type of strategy could also be an interesting alternative for the synthesis of lipophenols with shorter chains or those featuring saturated fatty acids. Indeed, it is highly likely that the yields of the last two coupling and deacylation steps would yield much better results with a different, shorter, and more linear fatty acid than DHA.

Chemical pathways: "butyrate" B1 and "acetate" B2. Despite the interesting three-step reduction offered by pathway **A** and the gram scale validation of the first four steps, this strategy is not suitable for large-scale synthesis due to the yield and the time-consuming nature of the two last steps. To achieve such goal, we decided to modify the previously reported chemical strategy[24] (involving transitory dioxole, then TIPS protection for the catechol moiety, and acetate protection for the 3, 5 and 7 phenolic positions). The major drawback of this strategy is the impossibility of scaling up the alkylation reaction, due to several intermolecular acetate migrations (Scheme 2). Such mobility of acetate groups, observed when basic conditions are used to introduce the isopropyl function, results in alkylation occurring at positions other than the 7 position. This also leads to the formation of monoalkylated, dialkylated, and triacetate by-products. The resulting mixture then requires tedious purification steps with either unreproducible yields on small scales (less than 500 mg), or the impossibility to isolate the desired product on large scales. To overcome this drawback two solutions were proposed. The first one involved replacing the acetate function with the bigger and less labile butyrate function (Scheme 3 pathway **B1**). The second relies on the use of intermolecular acetate migration during the alkylation reaction (Scheme 3 pathway **B2**).

"Butyrate" pathway B1. The butyrate protecting group had already been used for the synthesis of alkylated-resveratrol lipophenol.[24] Starting from dioxole quercetin **2**, positions 7, 5 and 3 were acylated using butyric anhydride (Scheme 3). The

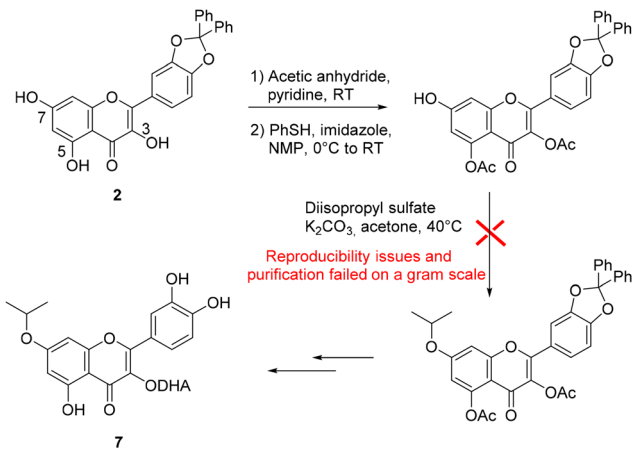

Scheme 2 Alkylation scale up issue in the previously reported quercetin-3-DHA-7-*i*Pr pathway.[24]

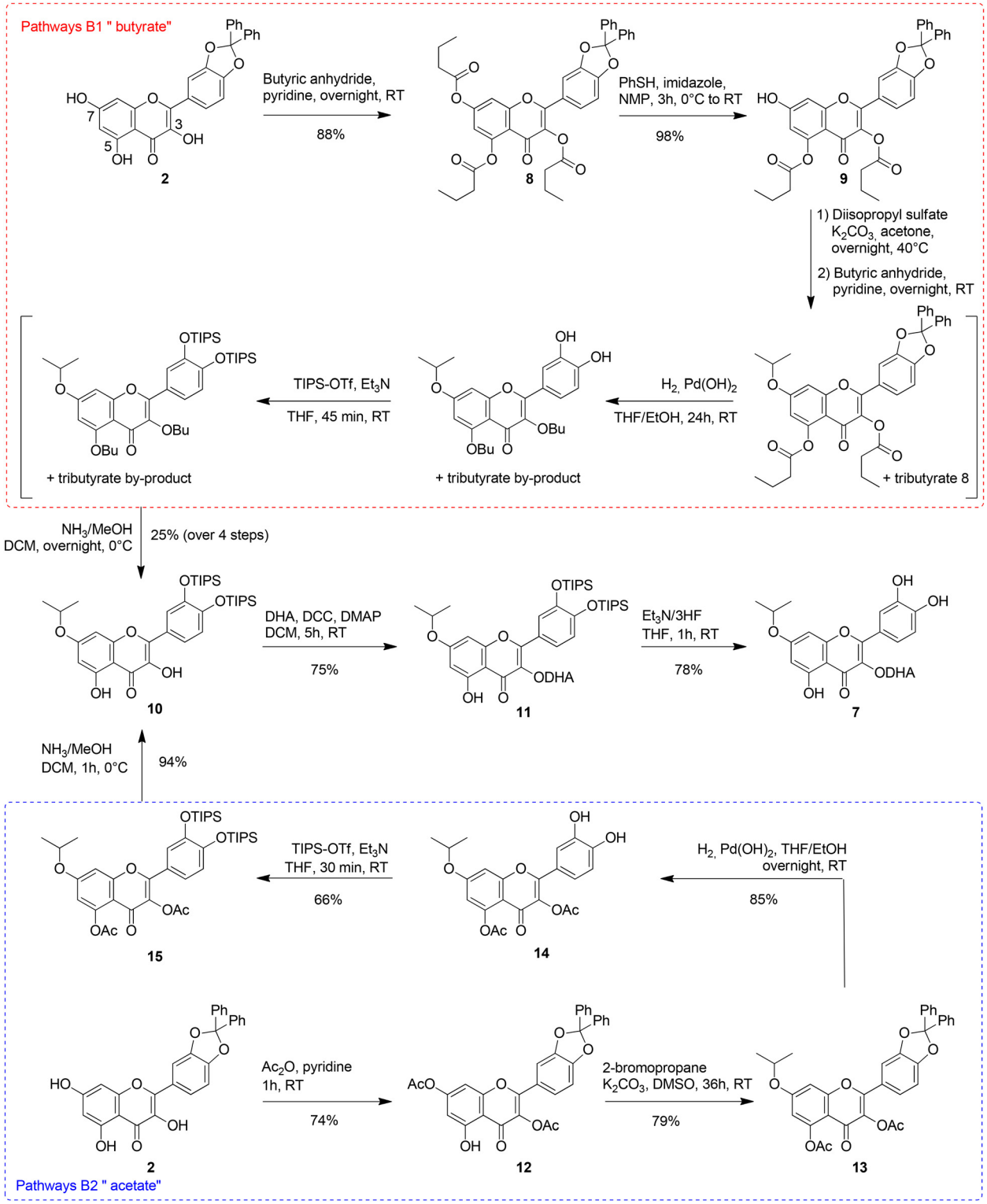

Scheme 3 Synthesis of quercetin-3-DHA-7-*i*Pr through **B1** "butyrate" and **B2** "acetate" protecting group strategies.

selective deprotection of the acetate at the 7 position was easily performed starting from tributyrate **8** in quantitative yield. Similar to acetate,[36] the reaction conditions with thiophenol/imidazole in the presence of *N*-methylpyrolidine did not deprotect positions 3 and 5 due to their lower acidity compared to OH-7. The tedious alkylation step was then carried out under basic conditions using diisopropyl sulfate from the mono-deprotected **9**. Unfortunately, migration of butyrate was

Table 2 Reproducibility of the "acetate" pathway **B2** on a gram scale

Synthesized compound	Reaction	Largest scale tested	Yield[a]	Reproducibility[b] n =	Average yield
2	Catechol protection	5 g	81%	5	71.2%
12	Di-acetylation	3.2 g	74%	6	74%
13	Isopropylation	3 g	79%	9	73.4%
14	Hydrogenation	2 g	85%	3	81.6%
15	TIPS introduction	2.3 g	66%	3	77%
10	De-acetylation	3.7 g	94%	4	93%
11	DHA coupling	3.1 g	75%	4	72.5%
7	TIPS removing	3 g	78%	5	80.2%

[a] On the largest scale. [b] Starting material > 1 g.

also observed during such alkylation, however, to a lesser extent. We only observed the migration of one butyrate leading to a monodeprotected quercetin as the major by-product. Unlike the previously reported pathway (Scheme 2), the reaction did not suffer from alkylation at other sites, allowing us to consider a larger scale reaction (5 g). After reintroduction of the labile butyrate, we obtained an inseparable mixture (Fig. S2†) of the desired alkylated quercetin at the 7 position and the tributyrate **8** derivative (Scheme 3). The following steps of the strategy, involving the dioxole catechol protecting group exchange with silylated protecting groups, were performed on the mixture. Only after deprotection of butyrate using ammonia solution, the remaining by-product could be easily removed, enabling alkyl compound **10** to be isolated in 25% yield over 5 steps. The final steps of the strategy were performed without scale-up issues, allowing first, the introduction of DHA only at the 3 position, facilitated by hydrogen bonding involving OH-5 (compound **11**), and then, subsequent catechol deprotection. TIPS were removed without the degradation of the bound ester or DHA. Following the validated pathway **B1**, 630 mg of quercetin-3-DHA-7-*i*Pr **7** could be obtained starting from 5 g of quercetin, with each reaction being carried out only once (Table 1). Pathway **B1** is thus an interesting strategy to access a gram scale reaction of alkyl quercetin lipophenol if it is performed at least twice. However, it needs an additional acylation step to solve butyrate migration issues during the alkylation process, and the selective deprotection at the 7 position is still performed using toxic PhSH/*N*-methylpyrolidine conditions that impose rigorous conditions during scale-up settings.

"Acetate" pathway B2. For an improved chemical strategy (with less steps, easier general work-up and less toxic reagents), we decided to use the restrictive intermolecular "acetate migration" as an advantage for isopropylation at the selective 7-position (pathway **B2** Scheme 3). Based on the work of Liu *et al.*[37] dioxole **2** was diacetylated on its two most reactive OH functions at the 7 and the 3 positions (compound **12**). Then, isopropylation was conducted using isopropyl bromide in the presence of K_2CO_3 and KI. The basic conditions of the reaction catalyzed an intermolecular cooperative migration of acetate, shifting it from the 7 position to the 5 position of **12**, liberating the 7 position only, for selective isopropylation. No by-products were formed in significant quantities during this process, enabling the isolation of isopropyl quercetin **13** without purification issues. The reaction was highly reproducible (Table 2), even on a gram scale (3 g). The end of the chemical pathway was adapted for the gram-scale reaction without significant changes in the chemical protocol. After hydrogenation, the dioxole group was replaced by TIPS (compound **15**) using TIPS triflate. The fatty acid DHA was then introduced at the 3-position, as previously explained, after acetate deprotection of **15**. After the reaction was performed, pathway **B2** allowed the isolation of 994 mg of lipophenol 7 (Table 1), with a global yield of 14.6% on height steps. It emerged as the best strategy for reproduction to access a gram amount of 7-alkyl quercetin lipophenol considering the number of steps, the global yield of the chemical synthesis (Table 1), and the purification process. Validation of the reproducibility on a gram scale (Tables 1 and 2) was realized on each step of strategy **B2** allowing us to isolate almost 3 grams of the desired compound **7**.

In vitro potency of quercetin-3-DHA-7-*i*Pr lipophenol against acrolein toxicity in neuroblastoma cells

The impact of quercetin-3-DHA-7-*i*Pr treatment on cell viability was assessed in human SH-SY5Y neuroblastoma cells with or without exposure to the carbonyl stress inducer acrolein. The activity of quercetin-3-DHA-7-*i*Pr (**7**) was compared with those of previously synthesized quercetin-7-*i*Pr, quercetin-3-DHA, commercial free DHA acid and quercetin (Fig. 2). As shown in Fig. 3A, the exposure of the cells to quercetin-3-DHA-7-*i*Pr (25 or 50 μM) for 24 h had no impact on cell viability. In contrast, viability did not exceed 50% when cells were exposed to quer-

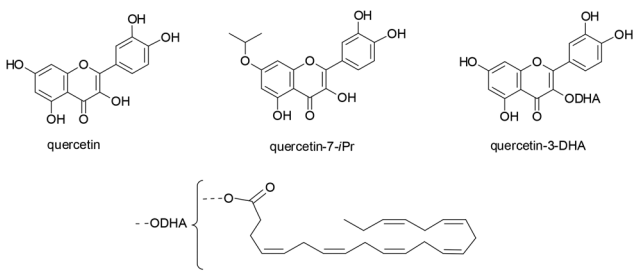

Fig. 2 Chemical structures of quercetin derivatives compared to that of quercetin-3-DHA-7-*i*Pr (**7**).

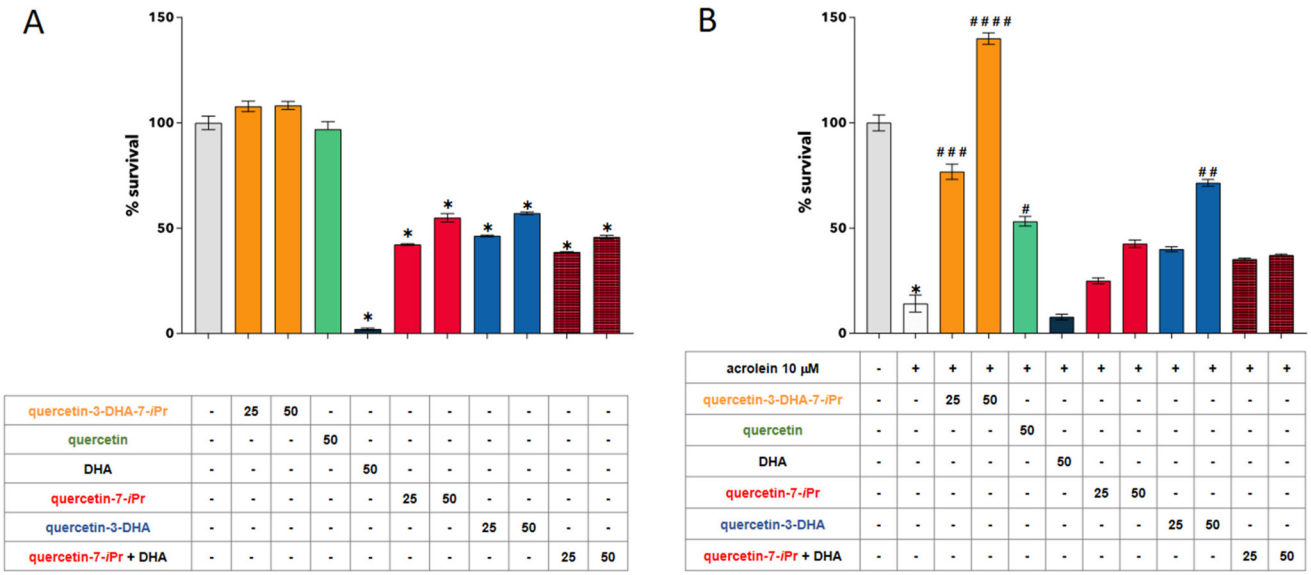

quercetin-3-DHA-7-*i*Pr	-	25	50	-	-	-	-	-	-	-	-
quercetin	-	-	-	50	-	-	-	-	-	-	-
DHA	-	-	-	-	50	-	-	-	-	-	-
quercetin-7-*i*Pr	-	-	-	-	-	25	50	-	-	-	-
quercetin-3-DHA	-	-	-	-	-	-	-	25	50	-	-
quercetin-7-*i*Pr + DHA	-	-	-	-	-	-	-	-	-	25	50

acrolein 10 µM	-	+	+	+	+	+	+	+	+	+	+
quercetin-3-DHA-7-*i*Pr	-	-	25	50	-	-	-	-	-	-	-
quercetin	-	-	-	-	50	-	-	-	-	-	-
DHA	-	-	-	-	-	50	-	-	-	-	-
quercetin-7-*i*Pr	-	-	-	-	-	-	25	50	-	-	-
quercetin-3-DHA	-	-	-	-	-	-	-	-	25	50	-
quercetin-7-*i*Pr + DHA	-	-	-	-	-	-	-	-	-	-	25	50

Fig. 3 Structure–function relationship of quercetin-3-DHA-7-*i*Pr on neuroblastoma cells: (A) effects of quercetin-3-DHA-7-*i*Pr (25 and 50 µM), quercetin (50 µM), DHA (50 µM), quercetin-7-*i*Pr (25 and 50 µM), quercetin-3-DHA (25 and 50 µM) and quercetin-7-*i*Pr + DHA (25 and 50 µM of each) on cell viability. SH-SY5Y cells were treated for 24 h with 25 and/or 50 µM of each compound in serum-free medium. Cell viability was determined using the MTT assay. The data are expressed as the percentage of control untreated cells and presented as mean ± SEM of two separate experiments; (B) neuroprotective effect of quercetin-3-DHA-7-*i*Pr against acrolein-induced toxicity. The cells were pre-treated for 2 h with quercetin-3-DHA-7-*i*Pr or other tested compounds at 25 and/or 50 µM (quercetin, DHA, quercetin-7-*i*Pr, quercetin-3-DHA and quercetin-7-*i*Pr + DHA) in serum-free medium before the addition of acrolein (10 µM) for 24 h. Cell viability was determined using the MTT assay. The data are expressed as the percentage of control untreated cells and presented as mean ± SEM of two separate experiments. * $p < 0.0001$ *versus* the control, # $p < 0.05$, # # $p < 0.01$, # # # $p < 0.001$, and # # # # $p < 0.0001$ (ANOVA test with Tukey's *post-hoc* analysis) *versus* the cells treated with acrolein.

cetin-7-*i*Pr, DHA, a combination of quercetin-7-*i*Pr + DHA, or quercetin-3-DHA. As shown in Fig. 3B, quercetin-3-DHA-7-*i*Pr (7) exhibited a dose-dependent, strong protective effect against acrolein-induced cell toxicity, and notably, this effect was much higher than the effects of quercetin, quercetin-7-*i*Pr and quercetin-3-DHA at the same concentration, indicating that both the isopropyl group and the DHA moiety of quercetin-3-DHA-7-*i*Pr are necessary to obtain a maximal protective effect under our experimental conditions. Interestingly, the highest concentration of quercetin-3-DHA-7-*i*Pr (7) resulted in higher cell viability than control conditions, showing an increase of around 30%. This may be explained by the fact that serum-free conditions induce oxidative stress, which can be counteracted when lipophenol is added to the culture medium during pre-incubation. The lack of protection observed during cell treatment with the quercetin-7-*i*Pr + DHA mixture underscores the significance of the covalent lipophenolic structure.

Retinopathies and neurodegenerative diseases have several common features such as the strong involvement of oxidative and carbonyl stresses in their etiology, and the presence of highly selective barriers that limit the diffusion of drugs to the eyes and brain, reducing their therapeutic efficacy. In previous studies conducted *in vitro* and *in vivo*, several lipophenols were demonstrated to efficiently protect retinal cells against *all-trans* retinal-induced carbonyl and oxidative stresses.[23–25] Our results are in line with these findings and extend the potential therapeutic benefits of lipophenols to neurodegenerative diseases such as AD. Interestingly, as previously observed with phloroglucinol-IP-DHA on ARPE-19 retinal cells,[24] the incorporation of the PUFA segment and the isopropyl moiety into quercetin was found to be essential for providing maximal cellular protection against carbonyl stressor toxicity. This could result from a significant improvement in quercetin lipophilicity and accretion to neuronal cells provided by the DHA graft, and/or from a synergistic effect arising from the alkyl phenol and DHA moieties. The exact mechanism underlying alkyl lipophenol protection against acrolein toxicity will be investigated in the near future, exploring two potential directions: direct aldehyde scavenging to reduce intracellular aldehyde concentration and/or the activation of aldehyde detoxification enzymes through the Nrf2-Keap1 pathway. The therapeutic potential of quercetin-3-DHA-7-*i*Pr will also be addressed *in vivo* using murine AD models.

Conclusion

Unlike chemical strategies for alkylated flavonoids involving the reconstruction of the three-ring skeleton of flavonoids starting from phloroglucinol building blocks,[38] we have successfully validated three new chemical strategies for 7-alkylated flavonoids using quercetin as the starting material. With this approach, the challenge was focused on the close reactivity of the different phenolic functions of quercetin. Considering the

biological relevance of the isopropyl function in carbonyl stress protection, the isopropylation reaction was carefully optimized to achieve maximum yield and good reproducibility on a gram scale either through a selection of an appropriate equivalent of an alkylated reagent (pathway **A**) or by utilizing the intra-molecular migration of acetate (pathway **B2**). The validation of the chemo-enzymatic pathways **A** highlighted the efficiency of supported lipase regioselective access to alkyl lipophenolic structures. This pathway, suitable for the small-scale synthesis of lipophenolic PUFA conjugates, allows for a reduction in the use of phenolic protecting groups and chemical steps. In the near future, it would be interesting to extrapolate this method to the synthesis of saturated lipophenols. Simultaneously, we have also confirmed the effectiveness of two additional strategies, which are better suited for scale-up synthesis. Notably, a final quantity of around 3 g of quercetin-3-DHA-7-*i*Pr was obtained through pathway **B2** (starting from around 15–20 g of quercetin), making it a validated strategy for future pre-clinical studies.

The cellular assay conducted in this study validated the protective effect of this isopropyl PUFA lipophenol against acrolein toxicity, a carbonyl stressor implicated in the physiopathology of neurodegenerative diseases, whether originating from environmental exposure or genetic predispositions (*via* oxidative stress). Given the beneficial role of quercetin lipophenol against carbonyl and reactive oxygen species toxicity, quercetin-3-DHA-7-*i*Pr emerges as an interesting candidate for further *in vivo* evaluation in mouse models of AD.

According to these *in vitro* results, the convergence of nutrition and organic chemistry paves the way for innovative solutions in the prevention and/or treatment of neurodegenerative pathologies such as AD. This opens new horizons to investigate deeper therapeutic developments based on lipophenols.

Experimental section

General methods

All solvents were anhydrous reagents from commercial sources. Unless otherwise noted, all chemicals and reagents were obtained commercially and used without purification. The reactions were monitored using TLC on plates that were pre-coated with silica gel 60 (Macherey-Nagel). The reaction components were visualized using a 254 nm UV lamp, stained with acidic *p*-anisaldehyde or $KMNO_4$ solution followed by gentle heating. Purifications of the synthesized compounds were performed by column chromatography on silica gel 40–63 μm. High-resolution mass spectra (HRMS) were recorded using a Q-Tof micro spectrometer (resolution 100 000, Waters) or mass spectrometers Synapt G2-S (Waters). Data were obtained by positive or negative electrospray ionization methods between 100 and 1500 Da by direct introduction (ESI, ASAP, FTMS + p APCI ionisation). NMR spectra were recorded at 300, 400 or 500 MHz (1H) and 75, 101 or 126 MHz (13C) using Bruker spectrometers. Chemical shifts are reported in parts per million (ppm, δ) relative to residual deuterated solvent peaks. The NMR spectra were assigned with the help of 2D NMR analyses (COSY, HSQC, and HMBC). The multiplicities reported are as follows: br = broad singlet, m = multiplet, s = singlet, d = doublet, t = triplet, q = quadruplet, quint = quintuplet, h = hextuple, or combinations thereof. For the peak assignments, the following abbreviations were used: Ar = aromatic, CH═CH = aliphatic alkene, and iP = isopropyl. If the reaction was performed several times, the protocol described is the one performed on the largest scale.

2-(2,2-Diphenylbenzo[*d*][1,3]dioxol-5-yl)-3,5,7-trihydroxy-4*H*-chromen-4-one (2). Anhydrous quercetin (**1**) (5.0 g, 16.8 mmol, 1 equiv.) was suspended in Ph_2O (150 mL) under N_2. Ph_2CCl_2 (4.55 mL, 23.7 mmol, 1.4 equiv.) was added to the suspension and the mixture was stirred at 180 °C for 4 hours. The mixture was then cooled to room temperature and poured into 400 mL cold pentane. The resulting suspension was filtered on Celite and washed with cold pentane to eliminate most of the Ph_2O. This process replaces the previously described centrifugation work-up.[24] The precipitate and Celite were gathered and mixed with 150 mL acetone. The mixture was stirred for 15 minutes to get all the solubilized product in acetone and was then filtered to remove Celite. The filtrate was recovered and the solvent was removed under reduced pressure to afford the crude product as a brown paste. The crude was then purified through silica gel column chromatography (solid deposit on Celite) with a pentane/EtOAc gradient of 90/10 to 70/30 as the eluent to yield the desired product **2** (6.35 g, 13.6 mmol, 81%) as a yellow solid. R_f = 0.6 (pentane/EtOAc 70 : 30); ^{1}H NMR (400 MHz, DMSO-d_6): δ 12.37 (s, 1H, OH_5), 10.87 (br, 1H, OH_7), 9.65 (br, 1H, OH_3), 7.84–7.78 (m, 2H, $H_{2'}$, $H_{6'}$), 7.58–7.56 (m, 4H, H_{Ar}), 7.49–7.42 (m, 6H, H_{Ar}), 7.22 (d, $^3J_{H,H}$ = 8.2 Hz, 1H, $H_{5'}$), 6.47 (d, $^4J_{H,H}$ = 2.0 Hz, 1H, H_8), 6.19 (d, $^4J_{H,H}$ = 2.0 Hz, 1H, H_6); ^{13}C NMR (75 MHz, DMSO-d_6): δ 176.0, 164.1, 160.7, 156.2, 147.6, 146.7, 145.6, 139.4 (2C), 136.4, 129.5 (2C), 128.6 (4C), 125.8 (4C), 125.2, 123.1, 117.1, 108.9, 107.8, 103.1, 98.3, 93.6; HRMS (ESI-TOF) *m*/*z*: calcd for $C_{28}H_{17}O_7$ $[M - H]^-$, 465.0974, found 465.0971.

3-(Benzyloxy)-2-(2,2-diphenylbenzo[*d*][1,3]dioxol-5-yl)-5,7-dihydroxy-4*H*-chromen-4-one (3a). To a solution of compound **2** (2.4 g, 5.15 mmol, 1.0 equiv.) in DMF (24 mL), benzyl bromide (818 μL, 6.69 mmol, 1.3 equiv.) and potassium carbonate (925 mg, 7.21 mmol, 1.4 equiv.) were added under N_2 at 0 °C. The reaction was monitored by TLC to validate the total conversion of the starting material (hardly eliminated during purification). The mixture was stirred overnight at room temperature. The resulting mixture was diluted with water (100 mL) and EtOAc (200 mL) and stirred at room temperature for 30 minutes. Then the organic layer was washed twice with H_2O (200 mL) and brine (100 mL) and dried over $MgSO_4$. The solvent was evaporated under reduced pressure and the residue was purified through silica gel column chromatography using spherical silica (liquid deposit) with a DCM/EtOAc gradient of 95/5 to 90/10. The desired monobenzylated compound **3a** was isolated as a pale yellow solid (1.66 g, 2.98 mmol, 58% yield). The dibenzylated by-product **3b** was also isolated as a thin yellow solid (1.05 g, 1.62 mmol, 32%

yield); **3a**: R_f = 0.5 (DCM/EtOAc 95 : 5); ^{1}H NMR (400 MHz, $CDCl_3$): δ 12.74 (s, 1H, OH_5), 7.61–7.59 (m, 4H, H_{Ar}), 7.56 (dd, $^3J_{H,H}$ = 8.4 Hz, $^4J_{H,H}$ = 1.8 Hz, 1H, $H_{6'}$), 7.49 (d, $^4J_{H,H}$ = 1.7 Hz, 1H, $H_{2'}$), 7.44–7.39 (m, 6H, H_{Ar}), 7.28–7.25 (m, 2H, H_{Ar}), 7.19–7.12 (m, 3H, H_{Ar}), 6.91 (d, $^3J_{H,H}$ = 8.4 Hz, 1H, $H_{5'}$), 6.37 (d, $^4J_{H,H}$ = 2.2 Hz, 1H, H_6 or H_8), 6.29 (d, $^4J_{H,H}$ = 2.2 Hz, 1H, H_6 or H_8), 5.90 (br, 1H, OH_7), 5.03 (s, 2H, CH_{2Bn}); ^{13}C NMR (126 MHz, $CDCl_3$): δ 179.0, 162.5, 162.3, 157.1, 157.0, 149.4, 147.4, 139.9 (2C), 137.2, 136.1, 129.5, 129.1, 128.5 (5C), 128.4, 128.3, 126.4 (6C), 124.3, 124.3, 117.9, 109.2, 108.5, 105.9, 99.3, 94.2, 74.7.

3,7-Bis(benzyloxy)-2-(2,2-diphenylbenzo[*d*][1,3]dioxol-5-yl)-5-hydroxy-4*H*-chromen-4-one (3b). R_f = 0.3 (DCM/EtOAc 98 : 2); ^{1}H NMR (400 MHz, $CDCl_3$): δ 12.68 (s, 1H, *OH*), 7.62–7.59 (m, 4H, H_{Ar}), 7.56 (dd, $^3J_{H,H}$ = 8.4 Hz, $^4J_{H,H}$ = 1.8 Hz, 1H, $H_{6'}$), 7.50 (d, $^4J_{H,H}$ = 1.7 Hz, 1H, $H_{2'}$), 7.44–7.34 (m, 12H, H_{Ar}), 7.28–7.26 (m, 1H, H_{Ar}), 7.21–7.13 (m, 3H, H_{Ar}), 6.91 (d, $^3J_{H,H}$ = 8.4 Hz, 1H, $H_{5'}$), 6.48 (d, $^4J_{H,H}$ = 2.2 Hz, 1H, H_6 or H_8), 6.44 (d, $^4J_{H,H}$ = 2.2 Hz, 1H, H_6 or H_8), 5.13 (s, 2H, CH_{2Bn}), 5.04 (s, 2H, CH_{2Bn}); ^{13}C NMR (126 MHz, $CDCl_3$): 178.9, 164.6, 162.2, 156.9 (2C), 149.4, 147.4, 139.9 (2C), 137.4, 136.3, 135.9, 129.5, 129.1, 128.9, 128.5 (8C), 128.3, 127.6, 126.4 (7C), 124.4, 124.2, 118.0, 109.2, 108.5, 106.3, 98.8, 93.2, 74.6, 70.6; HRMS (+ASAP) *m*/*z*: calcd for $C_{42}H_{31}O_7$: 647.2070 $[M + H]^+$, found: 647.2067.

3-(Benzyloxy)-2-(2,2-diphenylbenzo[*d*][1,3]dioxol-5-yl)-5-hydroxy-7-isopropoxy-4*H*-chromen-4-one (4a). Compound **3a** (1.2 g, 2.19 mmol, 1 equiv.) was dissolved in DMF (74 mL) under N_2. K_2CO_3 (1.21 g, 8.76 mmol, 4 equiv.), KI (1.45 g, 8.76 mmol, 4 equiv.) and 2-bromopropane (0.823 mL, 8.76 mmol, 4 equiv.) were added to the solution and the reaction was followed by TLC to avoid dialkylation. The mixture was stirred at room temperature for 28 hours. The solution was quenched with H_2O (200 mL), diluted with EtOAc (300 mL), and stirred for 30 min at room temperature. The organic layer was washed twice with H_2O (200 mL) and brine (50 mL). The organic layer was dried over $MgSO_4$ and the solvents were removed under reduced pressure. The crude was then purified through silica gel column chromatography (solid deposit) with a pentane/EtOAc gradient of 95/5 to 70/30 to yield the desired product **4a** (704 mg, 1.18 mmol, 53% (73% BSMR)) as a yellow solid. The dialkylated by-product **4b** was also isolated as a yellow solid (141 mg, 0.22 mmol, 10% yield); *increase in the reaction time, temperature, or the use of more than* 4 *eq. enhances the reactivity of OH-*5 *leading to the production of more dialkylated by products.* **4a**: R_f = 0.5 (pentane/EtOAc 9 : 1); **^{1}H NMR (400 MHz, $CDCl_3$)**: δ 12.64 (s, 1H, *OH*), 7.61–7.59 (m, 4H, H_{Ar}), 7.56 (dd, $^3J_{H,H}$ = 8.3 Hz, $^4J_{H,H}$ = 1.8 Hz, 1H, $H_{6'}$), 7.50 (d, $^4J_{H,H}$ = 1.7 Hz, 1H, $H_{2'}$), 7.44–7.39 (m, 6H, H_{Ar}), 7.28–7.26 (m, 2H, H_{Ar}), 7.21–7.13 (m, 3H, H_{Ar}), 6.91 (d, $^3J_{H,H}$ = 8.3 Hz, 1H, $H_{5'}$), 6.37 (d, $^4J_{H,H}$ = 2.2 Hz, 1H, H_6 or H_8), 6.33 (d, $^4J_{H,H}$ = 2.2 Hz, 1H, H_6 or H_8), 5.04 (s, 2H, CH_{2Bn}), 4.61 (sept, $^3J_{H,H}$ = 6.0 Hz, 1H, $CH_{i\text{-}Pr}$), 1.38 (d, $^3J_{H,H}$ = 6.0 Hz, 6H, $CH_{3i\text{-}Pr}$); **^{13}C NMR (126 MHz, $CDCl_3$)**: δ 178.9, 164.1, 162.2, 157.0, 156.7, 149.4, 147.4, 140.0 (2C), 137.3, 136.4, 129.5, 129.1, 128.5 (6C), 128.3, 126.4 (7C), 124.2, 117.9, 109.5, 108.5, 105.9, 99.1, 93.6, 74.6, 70.9, 22.1 (2C); **HRMS (+ASAP)** ***m*/*z***: calcd for $C_{38}H_{31}O_7$: 599.2070 $[M + H]^+$, found: 599.2074.

3-(Benzyloxy)-2-(2,2-diphenylbenzo[*d*][1,3]dioxol-5-yl)-5,7-diisopropoxy-4*H*-chromen-4-one (4b). R_f = 0.35 (pentane/EtOAc 70 : 30); ^{1}H NMR (400 MHz, $CDCl_3$): δ 7.60–7.58 (m, 4H, H_{Ar}), 7.52 (dd, $^3J_{H,H}$ = 8.3 Hz, $^4J_{H,H}$ = 1.8 Hz, 1H, $H_{6'}$), 7.48 (d, $^4J_{H,H}$ = 1.7 Hz, 1H, $H_{2'}$), 7.43–7.38 (m, 6H, H_{Ar}), 7.30–7.27 (m, 2H, H_{Ar}), 7.16–7.10 (m, 3H, H_{Ar}), 6.87 (d, $^3J_{H,H}$ = 8.3 Hz, 1H, $H_{5'}$), 6.42 (d, $^4J_{H,H}$ = 2.2 Hz, 1H, H_6 or H_8), 6.33 (d, $^4J_{H,H}$ = 2.2 Hz, 1H, H_6 or H_8), 5.05 (s, 1H, CH_{2Bn}), 4.61 (sept, $^3J_{H,H}$ = 6.0 Hz, 2H, $CH_{i\text{-}Pr}$), 1.48 (d, $^3J_{H,H}$ = 6.0 Hz, 6H, $CH_{3i\text{-}Pr}$), 1.39 (d, $^3J_{H,H}$ = 6.0 Hz, 6H, $CH_{3i\text{-}Pr}$); ^{13}C NMR (126 MHz, $CDCl_3$): δ 174.0, 162.1, 159.8, 159.0, 153.4, 148.7, 147.2, 140.1 (2C), 139.5, 137.1, 129.4, 129.1, 128.5 (5C), 128.1, 127.9, 126.4 (6C), 125.0, 123.6, 117.6, 110.4, 109.0, 108.3, 100.4, 94.1, 74.3, 72.6, 70.7, 22.1 (4C); HRMS (+ASAP) *m*/*z*: calcd for $C_{41}H_{37}O_7$: 641.2539 $[M + H]^+$, found: 641.2537.

2-(3,4-Dihydroxyphenyl)-3,5-dihydroxy-7-isopropoxy-4*H*-chromen-4-one (5). To a solution of compound **4a** (1.45 g, 2.43 mmol) in a mixture of anhydrous THF and absolute EtOH (53 : 27 mL, v/v), 20% palladium hydroxide (50% w/w, 727 mg) was added. The resulting mixture was stirred at room temperature under an H_2 atmosphere for 24 hours. Palladium hydroxide was removed by filtration on Celite and washed with EtOH. The filtrate was concentrated under reduced pressure. Purification of the residue was performed by silica gel column chromatography using DCM/MeOH (95/5) to give compound **5** (810 mg, 2.4 mmol, 98% yield) as a yellow solid. R_f = 0.5 (DCM/MeOH 95 : 5); ^{1}H NMR (400 MHz, $CDCl_3$): δ 7.75 (d, $^4J_{H,H}$ = 2.1, 1H, $H_{2'}$), 7.65 (dd, $^3J_{H,H}$ = 8.5 Hz, $^4J_{H,H}$ = 2.1 Hz, 1H, $H_{6'}$), 6.95 (d, $^3J_{H,H}$ = 8.5 Hz, 1H, $H_{5'}$), 6.43 (d, $^3J_{H,H}$ = 2.2 Hz, 1H, H_8 or H_6), 6.31 (d, $^3J_{H,H}$ = 2.2 Hz, 1H, H_8 or H_6), 4.62 (sept, $^2J_{H,H}$ = 6.1 Hz, 1H, $CH_{i\text{-}Pr}$), 1.37 (d, $^3J_{H,H}$ = 6.1 Hz, 6H, $CH_{3i\text{-}Pr}$); ^{13}C NMR (75 MHz, DMSO-d_6): 175.9, 163.2, 160.5, 156.2, 147.8, 147.2, 145.1, 136.0, 121.9, 120.0, 115.5, 115.3, 103.8, 98.4, 92.9, 70.4, 21.7 (2C); HRMS (ESI-TOF) *m*/*z*: calcd for $C_{18}H_{15}O_7$ $[M - H]^-$ 343.0818, found 343.0816.

4-(3-(((4*Z*,7*Z*,10*Z*,13*Z*,16*Z*,19*Z*)-Docosa-4,7,10,13,16,19-hexaenoyl)oxy)-5-hydroxy-7-isopropoxy-4-oxo-4*H*-chromen-2-yl)-1,2-phenylene (4*Z*,4′*Z*,7*Z*,7′*Z*,10*Z*,10′*Z*,13*Z*,13′*Z*,16*Z*,16′*Z*,19*Z*,19′*Z*)-bis(docosa-4,7,10,13,16,19-hexaenoate) (6). To a solution of compound **5** (150 mg, 0.43 mmol, 1.0 equiv.) in anhydrous DCM (30 mL) and DMF (1 mL), a solution of docosahexaenoic acid (402.2 mg, 1.22 mmol, 2.8 equiv.) was added in anhydrous DCM (2 × 5 mL) under N_2. Then, EDCI (234.7 mg, 1.22 mmol, 2.8 equiv.) and DMAP (26.7 mg, 0.22 mmol, 0.5 equiv.) were added to the reaction mixture. The resulting mixture was stirred at room temperature for 24 hours. The reaction was quenched with water (75 mL) and $NaHCO_3$ (25 mL). The aqueous layer was extracted with DCM (30 mL) twice. The organic layer was then washed twice with H_2O (125 mL) and saturated $NaHCO_3$ (25 mL), dried over $MgSO_4$, filtered and evaporated under reduced pressure. Purification of the resulting residue was performed by silica gel column chromatography (solid deposit on silica) using a DCM/pentane gradient of 80/20 to 100/0 to give compound **6** (122.5 mg, 0.09 mmol,

22% yield) as a dark yellow oil. A mixture of quercetin di-DHA-*i*Pr was also recovered (214 mg, 0.22 mmol, 52%). R_f = 0.5 (DCM/pentane 80 : 20); ^{1}H NMR (400 MHz, CD_3OD): δ 12.05 (s, 1H, *OH*), 7.71 (dd, $^3J_{H,H}$ = 8.5 Hz, $^4J_{H,H}$ = 2.1 Hz, 1H, $H_{6'}$), 7.79 (d, $^4J_{H,H}$ = 2.1, 1H, $H_{2'}$); 7.33 (d, $^3J_{H,H}$ = 8.5 Hz, 1H, $H_{5'}$), 6.43 (d, $^4J_{H,H}$ = 2.2 Hz, 1H, H_6 or H_8), 6.36 (d, $^4J_{H,H}$ = 2.2 Hz, 1H, H_6 or H_8), 5.51–5.27 (m, 36H, C*H*=C*H*$_{DHA}$), 4.63 (sept, $^3J_{H,H}$ = 6.0 Hz, 1H, C*H*$_{i\text{-}Pr}$), 2.89–2.79 (m, 30H, C*H*$_{2DHA(bis\text{-}allylic)}$), 2.72–2.62 (m, 6H, CO–C*H*$_{2DHA}$), 2.54–2.48 (m, 6H, CO–CH$_2$–C*H*$_{2DHA}$), 2.10–2.03 (m, 6H, CH$_3$–C*H*$_{2DHA}$), 1.38 (d, $^3J_{H,H}$ = 6.0 Hz, 6H, C*H*$_{3i\text{-}Pr}$), 0.99–0.94 (m, 9H, C*H*$_{3DHA}$); ^{13}C NMR (126 MHz, DMSO-d$_6$): δ 175.8, 170.4, 170.2, 170.1, 164.7, 162.1, 157.3, 154.7, 144.5, 142.3, 132.2 (2C), 132.2, 130.2 (3C), 129.9, 128.7 (3C), 128.7(3C), 128.4(5C), 128.4, 128.3, 128.2, 128.2, 128.1 (5C), 128.0, 128.0 (2C), 127.9, 127.6, 127.3, 127.3, 127.2, 127.1 (3C), 126.7, 124.0, 124.0, 105.5, 99.7, 94.1, 71.1, 34.1, 34.1, 33.7, 25.8 (14C), 25.7, 22.7(3C), 22.0 (2C), 20.7 (3C), 14.4 (3C); HRMS (FTMS + p APCI) *m*/*z*: calcd for $C_{84}H_{107}O_{10}$ $[M - H]^-$ 1275.78588, found 1275.78622.

(4*Z*,7*Z*,10*Z*,13*Z*,16*Z*,19*Z*)-5-Hydroxy-2-(3,4-dihydroxyphenyl)-7-isopropoxy-4-oxo-4*H*-chromen-3-yl docosa-4,7,10,13,16,19-hexaenoate (7)

*From pathway **A**.* To a solution of compound **6** (100 mg, 0.08 mmol) (or the mixture of quercetin di-DHA-*i*Pr (198 mg)) in *tert*-butylmethylether (13.4 mL), *n*-BuOH (0.50 mL) and supported Lipozyme® from *Mucor miehei* (1 : 1 w/w, 200 mg) were added. The resulting mixture was stirred at 40 °C for 8 days, after which the supported enzyme was filtrated and rinsed several times with DCM. The filtrate was concentrated under reduced pressure. Purification of the residue was performed by silica gel column chromatography (solid deposit) using a pentane/EtOAc gradient of 95/5 to 90/10 to give the desired product **7** (13 mg, 0.02 mmol, 26% from **6**; 36 mg, 0.05 mmol, 27% from the di-DHA mixture, and 19% from **5**) as a yellow solid.

*From pathway **B1** and **B2**.* The synthesis was realized starting from **11** (3.08 g, 3.14 mmol) as described by Moine *et al.*[24] and yielded **7** (1.61 g, 2.45 mmol, 78%) as a yellow solid. R_f = 0.5 (DCM/MeOH 95 : 5); ^{1}H NMR (400 MHz, $CDCl_3$): δ 12.13 (s, 1H, OH_5), 7.36–7.34 (m, 2H, $H_{6'}$, $H_{2'}$); 6.95 (d, $^3J_{H,H}$ = 9.0 Hz, 1H, $H_{5'}$), 6.41 (d, $^4J_{H,H}$ = 2.1 Hz, 1H, H_6 or H_8), 6.34 (d, $^4J_{H,H}$ = 2.1 Hz, 1H, H_6 or H_8), 5.89 (br, 2H, $OH_{3',4'}$), 5.47–5.41 (m, 12H, C*H*=C*H*$_{DHA}$), 4.62 (sept, $^3J_{H,H}$ = 6.0 Hz, 1H, C*H*$_{i\text{-}Pr}$), 2.94–2.76 (m, 10H, C*H*$_{2DHA(bis\ allylic)}$), 2.74–2.63 (m, 2H, CO–C*H*$_{2DHA}$), 2.57–2.46 (m, 2H, CO–CH$_2$–C*H*$_{2DHA}$), 2.12–2.01 (m, 2H, CH$_3$–C*H*$_{2DHA}$), 1.38 (d, $^3J_{H,H}$ = 6.0 Hz, 6H, C*H*$_{3i\text{-}Pr}$), 0.99–0.93 (m, 3H, C*H*$_{3DHA}$); ^{13}C NMR (126 MHz, $CDCl_3$): δ 175.9, 171.1, 164.6, 161.9, 157.2, 156.7, 147.5, 143.8, 132.2, 130.8, 130.0, 128.7, 128.6, 128.5 (2C), 128.2 (2C), 128.1, 128.0, 127.5, 127.2, 122.2, 121.9, 115.4, 115.2, 105.2, 99.6, 94.1, 71.1, 34.0, 25.8 (4C), 25.7, 22.7, 22.0 (2C), 20.7, 14.4; HRMS (ESI+) *m*/*z* calcd for $C_{40}H_{46}O_8$ $[M + H]^+$ 655.3265, found 655.3273.

2-(2,2-Diphenylbenzo[*d*][1,3]dioxol-5-yl)-4-oxo-4*H*-chromene-3,5,7-triyl tributyrate (8). Compound **2** (4.2 g, 9.01 mmol, 1 equiv.) was dissolved in pyridine (24 mL) under N_2. Butyric anhydride (8.85 mL, 54.0 mmol, 6 equiv.) was added to the solution and the mixture was stirred at room temperature overnight. The mixture was then quenched with 120 mL distilled water and extracted with 2 × 100 mL EtOAc. The organic layers were gathered, washed with 1 M HCl (2 × 100 mL), water (100 mL) and brine, and dried over $MgSO_4$. Solvents were removed under reduced pressure to yield the desired product **8** (5.37 g, 7.94 mmol, 88%) as a white solid, without the need for further purification. R_f = 0.9 (DCM/MeOH 96 : 4); ^{1}H NMR (500 MHz, $CDCl_3$): δ 7.60–7.55 (m, 4H, H_{Ar}), 7.44–7.38 (m, 7H, H_{Ar}), 7.36 (d, $^4J_{H,H}$ = 1.7 Hz, 1H, $H_{2'}$), 7.28 (d, $^4J_{H,H}$ = 2.2 Hz, 1H, H_8), 6.97 (d, $^3J_{H,H}$ = 8.3 Hz, 1H, $H_{5'}$), 6.83 (d, $^4J_{H,H}$ = 2.2 Hz, 1H, H_6), 2.71 (t, $^3J_{H,H}$ = 7.5 Hz, 2H, C$H_{2butyrate}$), 2.57 (t, $^3J_{H,H}$ = 7.3 Hz, 2H, C$H_{2butyrate}$), 2.57 (t, $^3J_{H,H}$ = 7.4 Hz, 2H, C$H_{2butyrate}$), 1.87–1.74 (m, 4H, 2 C$H_{2butyrate}$), 1.72 (q, $^3J_{H,H}$ = 7.4 Hz, 2H, C$H_{2butyrate}$), 1.05 (t, $^3J_{H,H}$ = 7.4 Hz, 3H, C$H_{3butyrate}$), 1.05 (t, $^3J_{H,H}$ = 7.4 Hz, 3H, C$H_{3butyrate}$), 0.94 (t, $^3J_{H,H}$ = 7.4 Hz, 3H, C$H_{3butyrate}$); ^{13}C NMR (126 MHz, $CDCl_3$): δ 172.1, 170.8, 170.7, 170.2, 157.0, 155.2, 154.3, 150.6, 149.9, 147.7, 139.7 (2C), 133.5, 129.6 (2C), 128.5 (4C), 126.4 (4C), 123.7, 123.3, 118.3, 114.9, 113.9, 108.9, 108.8, 108.6, 36.3, 36.1, 35.9, 18.4 (2C), 18.1, 13.8, 13.7, 13.7; HRMS (+ESI) *m*/*z*: calcd for $C_{40}H_{37}O_{10}$: 677.2381 $[M + H]^+$, found: 677.2568.

2-(2,2-Diphenylbenzo[*d*][1,3]dioxol-5-yl)-7-hydroxy-4-oxo-4*H*-chromene-3,5-diyl dibutyrate (9). Compound **8** (4.37 g, 6.46 mmol, 1 equiv.) was dissolved in NMP (100 mL) under N_2 and cooled to 0 °C. Imidazole (154 mg, 2.26 mmol, 0.35 equiv.) and PhSH (789 µL, 7.75 mmol, 1.2 equiv.) were added to the solution and the mixture was stirred at room temperature for 3 hours. The mixture was then cooled to 0 °C, quenched slowly with 3 M HCl and extracted with 2 × 100 mL EtOAc. The organic layers were gathered, washed with 1 M HCl (2 × 100 mL), distilled water (2 × 100 mL) and brine, and dried over $MgSO_4$. The crude was then purified through silica gel column chromatography with a DCM/MeOH gradient of 100/0 to 98/2 as the eluent to yield the desired product **9** (3.84 g, 6.33 mmol, 98%) as a light yellow solid. R_f = 0.2 (DCM/MeOH 98 : 2); ^{1}H NMR (500 MHz, $CDCl_3$): δ 7.94 (br, 1H, O*H*) 7.60–7.55 (m, 4H, H_{Ar}), 7.43–7.33 (m, 8H, H_{Ar}), 6.91 (d, $^3J_{H,H}$ = 8.7 Hz, 1H, $H_{5'}$), 6.56 (d, $^4J_{H,H}$ = 2.3 Hz, 1H, H_8), 6.43 (d, $^4J_{H,H}$ = 2.3 Hz, 1H, H_6), 2.68 (t, $^3J_{H,H}$ = 7.4 Hz, 2H, C$H_{2butyrate}$), 2.56 (t, $^3J_{H,H}$ = 7.4 Hz, 2H, C$H_{2butyrate}$), 1.77 (q, $^3J_{H,H}$ = 7.4 Hz, 2H, C$H_{2butyrate}$), 1.69 (q, $^3J_{H,H}$ = 7.4 Hz, 2H, C$H_{2butyrate}$), 0.91 (t, $^3J_{H,H}$ = 7.4 Hz, 3H, C$H_{3butyrate}$), 0.99 (t, $^3J_{H,H}$ = 7.4 Hz, 3H, C$H_{3butyrate}$); ^{13}C NMR (126 MHz, $CDCl_3$): δ 172.9, 171.9, 170.5, 161.5, 157.8, 155.0, 150.7, 149.8, 147.7, 139.8 (2C), 132.7, 129.6 (2C), 128.5 (4C), 126.4 (4C), 123.8, 123.4, 118.3, 110.5, 109.3, 108.7, 108.6, 101.4, 36.1, 36.0, 18.3, 18.1, 13.8, 13.6; HRMS (+ESI) *m*/*z*: calcd for $C_{36}H_{31}O_9$: 607.1963 $[M + H]^+$, found: 607.1952.

2-(3,4-Bis((triisopropylsilyl)oxy)phenyl)-3,5-dihydroxy-7-isopropoxy-4*H*-chromen-4-one (10)

*From pathway **B1** (in 5 steps from **9**).* Compound **9** (5.0 g, 8.24 mmol, 1 equiv.) was dissolved in acetone (400 mL) under N_2. K_2CO_3 (2.28 g, 16.5 mmol, 2 equiv.) and diisopropyl sulfate (2.73 mL, 16.5 mmol, 2 equiv.) were added to the solution and the mixture was stirred at 40 °C overnight. The mixture was

then filtered on Celite and the filtrate was mostly evaporated and dissolved in 150 mL DCM. The organic layer was washed with brine, dried over $MgSO_4$ and the solvents were removed under reduce pressure to afford the crude product as a yellow oil. The crude was then purified through silica gel column chromatography with a pentane/EtOAc gradient of 90/10 to 80/20 as the eluent. The fractions containing the desired product and the major by-products were gathered and solvents were evaporated to afford 4.26 g of a white solid. The solid was dissolved in pyridine (20 mL) under N_2. Butyric anhydride (1.8 mL, 11 mmol) was added and the mixture was stirred at room temperature overnight. The mixture was then quenched with 100 mL distilled water and extracted with 2 × 100 mL EtOAc. The organic layers were gathered, washed with 1 M HCl (100 mL), water (100 mL) and brine, and dried over $MgSO_4$. Solvents were removed under reduced pressure to afford the crude product as yellow oil. The crude was then purified through silica gel column chromatography with a pentane/EtOAc gradient of 90/10 to 80/20 as the eluent to yield an unseparable mixture of compounds **S1** and tributyrate by-product **8** as a white solid (3.91 g), in 57/43 proportion estimated using ^{1}H NMR integration of the $H_{6/8}$ signal. **S1**: R_f = 0.4 (cyclohexane/EtOAc 80 : 20); a mixture of compound **S1** and by-product **8** (3.1 g) was dissolved in THF/EtOH (77/33 mL) and $Pd(OH)_2$ (20 wt%, 620 mg) was added. The mixture was stirred vigorously under an H_2 atmosphere for 24 hours. The mixture was then filtered on Celite and the solvents were evaporated to afford the crude product as a green paste. The crude was then purified through silica gel column chromatography with a DCM/MeOH gradient of 100/0 to 96/4 as the eluent to yield an inseparable mixture of the desired product **S2** and its tributyrated by-product (1.9 g) as a yellow solid, in 58/42 proportion estimated using ^{1}H NMR integration of the $H_{5'}$ signal. **S2**: R_f = 0.25 (DCM/MeOH, 96 : 4); the previously mentioned mixture of **S2** (1.9 g) was dissolved in dry THF (50 mL). Distilled Et_3N (2.19 mL, 15.7 mmol) and TIPSOTf (2.37 mL, 8.63 mmol) were added and the mixture was stirred at room temperature for 45 minutes. The mixture was then quenched with 50 mL distilled water and extracted with EtOAc (2 × 50 mL). The gathered organic phases were washed with 1 M HCl (50 mL) and brine, dried over $MgSO_4$ and the solvents were removed under reduced pressure to afford the crude product as yellow oil. The crude was then purified through silica gel column chromatography with a pentane/EtOAc gradient of 80/20 as the eluent to yield an inseparable mixture of compounds **S3** and its tributyrated by-product as yellow oil (2.77 g), in 61/39 proportion estimated using ^{1}H NMR integration of the $H_{6/8}$ signal. **S3**: R_f = 0.4 (cyclohexane/EtOAc, 60 : 40); the previously mentioned mixture of **S3** (2.77 g) was dissolved in DCM/MeOH (28/15 mL) under N_2 and cooled to 0 °C. NH_3 (7 N in MeOH, 6 mL, 41.8 mmol, 12 equiv.) was added and the mixture was stirred at room temperature overnight. The mixture was then diluted with 100 mL DCM. The organic layer was washed with 1 M HCl (50 mL) and brine, dried over $MgSO_4$ and the solvents were removed under reduced pressure to afford the crude product as brown oil. The crude was then purified through silica gel column chromatography with a pentane/EtOAc gradient of 90/10 as the eluent to yield the pure desired product **10** (1.24 g, 1.89 mmol, 25% over 5 steps) as a brown solid.

*From pathway **B2** (in 1 step from **15**):.* The synthesis was realized starting from **15** (3.66 g, 4.94 mmol) as described by Moine *et al.*[24] and yielded **10** (3.06 g, 4.65 mmol, 95%) as a brownish solid. R_f = 0.4 (cyclohexane/EtOAc, 95 : 5); ^{1}H NMR (400 MHz, $CDCl_3$): δ 11.71 (s, 1H, OH_5), 7.83 (d, $^4J_{H,H}$ = 2.3 Hz, 1H, $H_{2'}$), 7.66 (dd, $^3J_{H,H}$ = 8.6 Hz, $^4J_{H,H}$ = 2.3 Hz, 1H, $H_{6'}$), 6.95 (d, $^3J_{H,H}$ = 8.6 Hz, 1H, $H_{5'}$), 6.56 (s, 1H, OH_3), 6.39 (d, $^4J_{H,H}$ = 2.1 Hz, 1H, H_8), 6.34 (d, $^4J_{H,H}$ = 2.1 Hz, 1H, H_6), 4.62 (hept, $^3J_{H,H}$ = 6.0 Hz, 1H, C$H_{i\text{-}Pr}$), 1.39 (d, $^3J_{H,H}$ = 6.0 Hz, 6H, 2 C$H_{3i\text{-}Pr}$), 1.38–1.29 (m, 6H, 6 CH_{TIPS}), 1.18–1.11 (m, 36H, 12 CH_{3TIPS}); ^{13}C NMR (126 MHz, $CDCl_3$) δ 175.2, 164.2, 161.0, 156.9, 149.4, 147.2, 145.7, 135.7, 123.5, 120.9, 120.0, 119.5, 103.7, 98.8, 93.7, 71.0, 22.1 (2C), 18.2 (6C), 18.1 (6C), 13.3 (3C), 13.1 (3C); HRMS (ESI-TOF) m/z calcd for $C_{36}H_{55}O_7Si_2$ $[M - H]^-$ 655.3486, found 655.3487.

(4*Z*,7*Z*,10*Z*,13*Z*,16*Z*,19*Z*)-5-Hydroxy-2-(3,4-ditriisopropylsilyloxyphenyl)-7-isopropoxy-4-oxo-4*H*-chromen-3-yl docosa-4,7,10,13,16,19-hexaenoate (11). The synthesis was realized starting from **10** (3.06 g, 4.66 mmol) as described by Moine *et al.*[24] and yielded **11** (3.40 g, 3.51 mmol, 75%) as yellow oil. R_f = 0.24 (pentane/DCM, 50 : 50); ^{1}H NMR (400 MHz, $CDCl_3$): δ 12.19 (s, 1H, OH_5), 7.39 (d, $^4J_{H,H}$ = 2.3 Hz, 1H, $H_{2'}$), 7.33 (dd, $^3J_{H,H}$ = 8.5 Hz, $^4J_{H,H}$ = 2.2 Hz, 1H, $H_{6'}$), 6.90 (d, $^3J_{H,H}$ = 8.5 Hz, 1H, $H_{5'}$), 6.36 (d, $^4J_{H,H}$ = 2.2 Hz, 1H, H_8), 6.34 (d, $^4J_{H,H}$ = 2.2 Hz, 1H, H_6), 5.51–5.24 (m, 12H, CH=CH_{DHA}) 4.61 (hept, $^3J_{H,H}$ = 6.0 Hz, 1H, C$H_{i\text{-}Pr}$), 2.89–2.78 (m, 10H, C$H_{2DHA(bis\ allylic)}$), 2.69 (t, $^3J_{H,H}$ = 7.6 Hz, 2H, CO–CH_{2DHA}), 2.51 (q, $^3J_{H,H}$ = 7.3 Hz, 2H, CO–CH$_2$–CH_{2DHA}), 2.07 (p, $^3J_{H,H}$ = 7.3 Hz, 2H, CH$_3$–CH_{2DHA}), 1.39 (d, $^3J_{H,H}$ = 6.0 Hz, 6H, 2 C$H_{3i\text{-}Pr}$), 1.36–1.29 (m, 6H, 6 CH_{TIPS}), 1.16–1.10 (m, 36H, 12 CH_{3TIPS}), 0.96 (t, $^3J_{H,H}$ = 7.5 Hz, 3H, CH_{3DHA}); ^{13}C NMR (101 MHz, $CDCl_3$): δ 175.9, 170.4, 164.4, 162.2, 157.2, 156.4, 150.5, 147.2, 132.2, 131.2, 129.8, 128.7, 128.5, 128.4 (2C), 128.3, 128.2, 128.2, 128.0, 127.7, 127.2, 122.2, 122.1, 119.9, 119.9, 105.3, 99.2, 94.0, 71.0, 33.9, 25.8 (4C), 25.7, 22.8, 22.0 (2C), 20.7, 18.1 (6C), 18.1 (6C), 14.4, 13.3 (3C), 13.2 (3C); HRMS (ASAP-TOF) calcd for $C_{58}H_{87}O_8Si_2$ $[M + H]^+$ 967.5939, found 967.5927.

2-(2,2-Diphenylbenzo[*d*][1,3]dioxol-5-yl)-5-hydroxy-4-oxo-4*H*-chromene-3,7-diyl diacetate (12). Compound **1** (3.2 g, 6.86 mmol, 1 equiv.) was dissolved in pyridine (30 mL) under N_2. Ac_2O (1.30 mL, 13.72 mmol, 2 equiv.) was added to the solution and the mixture was stirred at room temperature for 15 min. The mixture was then quenched with 150 mL distilled water and extracted with 2 × 100 mL EtOAc. The organic layers were gathered, washed with 1 M HCl (3 × 100 mL), water (100 mL) and brine and dried over $MgSO_4$. The crude was then purified through silica gel column chromatography (solid deposit) with a DCM/EtOAc gradient of 100/0 to 95/5 as the eluent to yield the desired product **2** (2.8 g, 5.09 mmol, 74%) as a pale yellow solid; R_f = 0.4 (cyclohexane/EtOAc, 70 : 30); ^{1}H NMR (400 MHz, $CDCl_3$): δ 12.21 (s, 1H, OH), 7.61–7.56 (m, 4H, H_{Ar}), 7.45 (dd, $^3J_{H,H}$ = 8.3 Hz, $^4J_{H,H}$ = 1.8 Hz, 1H, H_{Ar}), 7.43–7.38 (m, 7H, H_{Ar}), 7.00 (d, $^3J_{H,H}$ = 8.3 Hz, 1H, H_{Ar}), 6.82

(d, $^4J_{H,H}$ = 2.0 Hz, 1H, H_{Ar}), 6.58 (d, $^4J_{H,H}$ = 2.0 Hz, 1H, H_{Ar}), 2.36 (s, 3H, CH_{3Ac}), 2.33 (s, 3H, CH_{3Ac}); ^{13}C NMR (101 MHz, $CDCl_3$): δ 176.4, 168.4, 167.9, 161.8, 157.2, 156.3, 156.0, 150.3, 147.9, 139.6 (2C), 131.5, 129.6 (2C), 128.6 (4C), 126.4 (4C), 124.0, 123.0, 118.5, 109.0, 108.8, 108.5, 105.5, 101.2, 21.3, 20.7; HRMS (ESI-TOF) m/z calcd for $C_{32}H_{23}O_9$ $[M + H]^+$ 551.1342, found 551.1342.

2-(2,2-Diphenylbenzo[*d*][1,3]dioxol-5-yl)-7-isopropoxy-4-oxo-4*H*-chromene-3,5-diyl diacetate (13). Compound **12** (3.0 g, 5.45 mmol, 1 equiv.) was dissolved in DMSO (60 mL) under N_2. K_2CO_3 (830 mg, 6.00 mmol, 1.1 equiv.) and 2-bromopropane (1.54 mL, 16.20 mmol, 3 equiv.) were added to the solution and the mixture was stirred at room temperature for 40 hours. The mixture was then cooled to 0 °C and quenched with 100 mL H_2O. The mixture was extracted with 3 × 100 mL EtOAc, organic layers were gathered and washed with 0.5 M HCl, H_2O and brine. The organic layer was dried over $MgSO_4$ and the solvents were removed under reduced pressure. The crude was then purified through silica gel column chromatography (solid deposit on silica) with a pentane/EtOAc gradient of 90/10 to 70/30 as the eluent to yield the desired product **13** (2.5 g, 4.22 mmol, 79%) as a white solid; R_f = 0.2 (cyclohexane/EtOAc, 70 : 30); ^{1}H NMR (400 MHz, $CDCl_3$): δ 7.64–7.52 (m, 4H, H_{Ar}), 7.45–7.32 (m, 8H, H_{Ar}), 6.97 (d, $^3J_{H,H}$ = 8.2 Hz, 1H, H_{Ar}), 6.77 (d, $^4J_{H,H}$ = 2.4 Hz, 1H, H_{Ar}), 6.57 (d, $^4J_{H,H}$ = 2.4 Hz, 1H, H_{Ar}), 4.62 (hept, $^3J_{H,H}$ = 5.9 Hz, 1H, C$H_{i\text{-}Pr}$), 2.42 (s, 3H, CH_{3Ac}), 2.31 (s, 3H, CH_{3Ac}), 1.39 (d, $^3J_{H,H}$ = 6.0 Hz, 6H, 2 C$H_{3i\text{-}Pr}$); ^{13}C NMR (75 MHz, $CDCl_3$): δ 170.3, 169.8, 168.3, 162.3, 158.3, 154.7, 150.8, 149.7, 147.8, 139.8 (2C), 133.2, 129.6 (2C), 128.5 (4C), 126.4 (4C), 123.6, 123.3, 118.3, 110.7, 109.7, 108.8, 108.4, 100.0, 71.4, 21.9, 21.3, 20.9; HRMS (ESI-TOF) m/z: calcd for $C_{35}H_{29}O_9$ $[M + H]^+$ 593.1812, found 593.1801.

2-(3,4-Dihydroxyphenyl)-7-isopropoxy-4-oxo-4*H*-chromene-3,5-diyl diacetate (14). The procedure was adapted from the one previously described[24] to allow the scale up. Compound **13** (2 g, 3.38 mmol, 1 equiv.) was dissolved in THF/EtOH (68/32 mL) and 20% $Pd(OH)_2$ (20% w/w, 400 mg) was added. The reaction medium needs to be concentrated to enhance the reaction kinetics. The mixture was stirred vigorously under an H_2 atmosphere for 20 hours. In the presence of the remaining starting material on thin-layer chromatography (TLC) after an overnight reaction, the $Pd(OH)_2$ catalyst was replaced with a new amount of reagent, and the reaction was allowed to proceed for an additional 5 hours. The mixture was then filtered on Celite and the solvents were evaporated to afford the crude product as a green paste. Then, silica gel purification was promptly performed to minimize the migration of acetate groups. The crude was purified through silica gel column chromatography (liquid deposit) with a fast DCM/MeOH gradient of 100/0 to 96/4 as the eluent to yield the desired product **14** (1.22 g, 2.85 mmol, 85%) as a pale yellow solid. R_f = 0.2 (DCM/MeOH 96 : 4); ^{1}H NMR (400 MHz, DMSO-d_6): δ 9.65 (br, 2H, 2 OH), 7.34 (d, $^4J_{H,H}$ = 2.3 Hz, 1H, H_{Ar}), 7.29 (dd, $^3J_{H,H}$ = 8.4, $^4J_{H,H}$ = 2.3 Hz, 1H, H_{Ar}), 7.21 (d, $^4J_{H,H}$ = 2.4 Hz, 1H, H_{Ar}), 6.92 (d, $^3J_{H,H}$ = 8.4 Hz, 1H, H_{Ar}), 6.76 (d, $^4J_{H,H}$ = 2.4 Hz, 1H, H_{Ar}), 4.86 (hept, $^3J_{H,H}$ = 5.9 Hz, 1H, C$H_{i\text{-}Pr}$), 2.32 (s, 3H, CH_{3Ac}), 2.29 (s, 3H, CH_{3Ac}), 1.33 (d, $^3J_{H,H}$ = 6.0 Hz, 6H, 2 C$H_{3i\text{-}Pr}$); ^{13}C NMR (101 MHz, DMSO-d_6): δ 168.9, 168.8, 167.9, 161.7, 157.5, 154.3, 150.0, 149.0, 145.4, 131.7, 120.3, 119.7, 115.9, 115.0, 109.6, 109.4, 100.2, 71.0, 21.5 (2C), 20.9, 20.4; HRMS (ESI-TOF) m/z: calcd for $C_{22}H_{19}O_9$ $[M - H]^-$ 427.1029, found 427.1031.

3,5-Diacetyloxy-2-(3,4-ditriisopropylsilyloxyphenyl)-7-isopropoxy-4*H*-chromen-4-one (15). The synthesis was realized starting from **14** (2.32 g, 5.42 mmol) as described in Moine *et al.*[24] and yielded **15** (2.64 g, 3.56 mmol, 66%) as a white solid. R_f = 0.63 (pentane/EtOAc, 70 : 30); ^{1}H NMR (300 MHz, $CDCl_3$) δ 7.36 (d, $^4J_{H,H}$ = 2.3 Hz, 1H, $H_{2'}$), 7.30 (dd, $^3J_{H,H}$ = 8.5, $^4J_{H,H}$ = 2.3 Hz, 1H, $H_{6'}$), 6.91 (d, $^3J_{H,H}$ = 8.4 Hz, 1H, $H_{5'}$), 6.74 (d, $^4J_{H,H}$ = 2.5 Hz, 1H, H_8), 6.56 (d, $^4J_{H,H}$ = 2.5 Hz, 1H, H_6), 4.61 (hept, $^3J_{H,H}$ = 6.0 Hz, 1H, C$H_{i\text{-}Pr}$), 2.42 (s, 3H, CH_{3Ac}), 2.32 (s, 3H, CH_{3Ac}), 1.39 (d, $^3J_{H,H}$ = 6.0 Hz, 6H, 2 C$H_{3i\text{-}Pr}$), 1.38–1.27 (m, 6H, 6 CH_{TIPS}), 1.13 (d, $^3J_{H,H}$ = 7.3 Hz, 36H, 12 CH_{3TIPS}); ^{13}C NMR (101 MHz, $CDCl_3$) δ 170.4, 169.8, 168.2, 162.2, 158.3, 154.9, 150.8, 150.2, 147.1, 133.2, 122.3, 121.6, 120.0, 119.9, 110.7, 109.4, 100.1, 71.3, 21.9 (2C), 21.3, 20.8, 18.1 (6C), 18.1 (6C), 13.3 (3C), 13.2 (3C); HRMS (ESI-TOF) m/z: calcd for $C_{40}H_{61}O_9Si_2$ $[M + H]^+$ 741.3854, found 741.3849.

Cell culture experiments

SHSY-5Y cells (purchased from ATCC) were used at passage 15. They were cultured in DMEM/F12 medium supplemented with 10% FBS and 1% penicillin–streptomycin. For the experiments, the cells were plated and allowed to differentiate in 96-well plates at a density of 40 000 cells per well in DMEM/F12 medium supplemented with 3% FBS, 1% penicillin–streptomycin and 3.36 mM retinoic acid. After 72 h, they were rinsed with DPBS and pre-treated with various concentrations of DHA, quercetin, quercetin-7-*i*Pr or lipophenolic compounds for 2 h in serum-free DMEM/F12 medium before the addition of 10μM acrolein. Cell viability was determined after a 24-hour incubation using the MTT (3-[4,5-dimethylthiazol-2-yl]-2,5-diphenyltetrazolium bromide, Sigma-Aldrich) test. Briefly, MTT was dissolved at 0.5 mg mL^{-1} in PBS and added to the cells for 1 h. Then, the medium was discarded, replaced with DMSO, and the plate was placed on an orbital shaker for 1 h at room temperature to dissolve formazan crystals. A microplate reader (Multiskan Sky, Thermo Scientific) was used to measure the absorbance at 540 nm. The data are expressed as the percentage of control untreated cells and presented as mean ± SEM of two separate experiments. Statistical comparisons were performed using the ANOVA test with Tukey's *post-hoc* analysis.

Author contributions

LO, LM and JL carried out the chemical syntheses and analysed the products. LO conducted and evaluated all biological assays. JL, CD and CC wrote the manuscript. TD and LG supervised the project. CD and CC initiated, supervised the project and acquired financial support for the project.

Conflicts of interest

There are no conflicts to declare.

Acknowledgements

This research was funded by the University of Montpellier, the ANR (LipoPheRet - ANR-18-CE18-0017 and LabEx LIPSTIC - ANR-11-LABX-0021), the Région Bourgogne Franche-Comté, and the Fonds Européen de Développement Régional. CNRS and INSERM are thanked for their support.

References

1 S. Mani, R. Dubey, I.-C. Lai, M. A. Babu, S. Tyagi, G. Swargiary, D. Mody, M. Singh, S. Agarwal, D. Iqbal, S. Kumar, M. Hamed, P. Sachdeva, A. G. Almutary, H. M. Albadrani, S. Ojha, S. K. Singh and N. K. Jha, Oxidative Stress and Natural Antioxidants: Back and Forth in the Neurological Mechanisms of Alzheimer's Disease, *J. Alzheimer's Dis.*, 2023, **96**, 877–912.

2 M. Perluigi, F. Di Domenico and D. A. Butterfield, Oxidative damage in neurodegeneration: roles in the pathogenesis and progression of Alzheimer disease, *Physiol. Rev.*, 2024, **104**, 103–197.

3 T. I. Williams, B. C. Lynn, W. R. Markesbery and M. A. Lovell, Increased levels of 4-hydroxynonenal and acrolein, neurotoxic markers of lipid peroxidation, in the brain in Mild Cognitive Impairment and early Alzheimer's disease, *Neurobiol. Aging*, 2006, **27**, 1094–1099.

4 M. A. Lovell, C. Xie and W. R. Markesbery, Acrolein is increased in Alzheimer's disease brain and is toxic to primary hippocampal cultures, *Neurobiol. Aging*, 2001, **22**, 187–194.

5 M. J. Picklo, T. J. Montine, V. Amarnath and M. D. Neely, Carbonyl toxicology and Alzheimer's disease, *Toxicol. Appl. Pharmacol.*, 2002, **184**, 187–197.

6 Q. Liu, A. K. Raina, M. A. Smith, L. M. Sayre and G. Perry, Hydroxynonenal, toxic carbonyls, and Alzheimer disease, *Mol. Aspects Med.*, 2003, **24**, 305–313.

7 M. Singh, T. N. Dang, M. Arseneault and C. Ramassamy, Role of by-products of lipid oxidation in Alzheimer's disease brain: a focus on acrolein, *J. Alzheimer's Dis.*, 2010, **21**, 741–756.

8 S. M. Innis, Dietary (n-3) Fatty Acids and Brain Development12, *J. Nutr.*, 2007, **137**, 855–859.

9 R. J. S. Lacombe, M. E. Smith, K. Perlman, G. Turecki, N. Mechawar and R. P. Bazinet, Quantitative and carbon isotope ratio analysis of fatty acids isolated from human brain hemispheres, *J. Neurochem.*, 2023, **164**, 44–56.

10 N. G. Bazan, V. L. Marcheselli and K. Cole-Edwards, Brain response to injury and neurodegeneration: endogenous neuroprotective signaling, *Ann. N. Y. Acad. Sci.*, 2005, **1053**, 137–147.

11 H. N. Yassine, Q. Feng, I. Azizkhanian, V. Rawat, K. Castor, A. N. Fonteh, M. G. Harrington, L. Zheng, B. R. Reed, C. DeCarli, W. J. Jagust and H. C. Chui, Association of Serum Docosahexaenoic Acid With Cerebral Amyloidosis, *JAMA Neurol.*, 2016, **73**, 1208–1216.

12 M. Haution-Bitker, T. Gilbert, A. Vignoles, C. Lecardonnel, S. Watelet, E. Blond, J. Drai and M. Bonnefoy, Associations between Plasmatic Polyunsaturated Fatty Acids Concentrations and Cognitive Status and Decline in Neurocognitive Disorders, *J. Nutr., Health Aging*, 2018, **22**, 718–725.

13 R. P. Bazinet and S. Layé, Polyunsaturated fatty acids and their metabolites in brain function and disease, *Nat. Rev. Neurosci.*, 2014, **15**, 771–785.

14 I. M. Dighriri, A. M. Alsubaie, F. M. Hakami, D. M. Hamithi, M. M. Alshekh, F. A. Khobrani, F. E. Dalak, A. A. Hakami, E. H. Alsueaadi, L. S. Alsaawi, S. F. Alshammari, A. S. Alqahtani, I. A. Alawi, A. A. Aljuaid and M. Q. Tawhari, Effects of Omega-3 Polyunsaturated Fatty Acids on Brain Functions: A Systematic Review, *Cureus*, 2022, **14**, e30091.

15 B. Troesch, M. Eggersdorfer, A. Laviano, Y. Rolland, A. D. Smith, I. Warnke, A. Weimann and P. C. Calder, Expert Opinion on Benefits of Long-Chain Omega-3 Fatty Acids (DHA and EPA) in Aging and Clinical Nutrition, *Nutrients*, 2020, **12**, 2555.

16 C. Zussy, R. John, T. Urgin, L. Otaegui, C. Vigor, N. Acar, G. Canet, M. Vitalis, F. Morin, E. Planel, C. Oger, T. Durand, S. L. Rajshree, L. Givalois, P. V. Devarajan and C. Desrumaux, Intranasal Administration of Nanovectorized Docosahexaenoic Acid (DHA) Improves Cognitive Function in Two Complementary Mouse Models of Alzheimer's Disease, *Antioxidants*, 2022, **11**, 838.

17 C. H. Maclean, A. M. Issa, S. J. Newberry, W. A. Mojica, S. C. Morton, R. H. Garland, L. G. Hilton, S. B. Traina and P. G. Shekelle, Effects of omega-3 fatty acids on cognitive function with aging, dementia, and neurological diseases, *Evid. Rep. Technol. Assess*, 2005, 1–3.

18 S. Śliwińska and M. Jeziorek, The role of nutrition in Alzheimer's disease, *Rocz. Panstw. Zakl. Hig.*, 2021, **72**, 29–39.

19 S. Quideau, D. Deffieux, C. Douat-Casassus and L. Pouységu, Plant polyphenols: chemical properties, biological activities, and synthesis, *Angew. Chem., Int. Ed.*, 2011, **50**, 586–621.

20 Q. Zhu, Z. P. Zheng, K. W. Cheng, J. J. Wu, S. Zhang, Y. S. Tang, K. H. Sze, J. Chen, F. Chen and M. Wang, Natural polyphenols as direct trapping agents of lipid peroxidation-derived acrolein and 4-hydroxy-trans-2-nonenal, *Chem. Res. Toxicol.*, 2009, **22**, 1721–1727.

21 X. Shao, H. Chen, Y. Zhu, R. Sedighi, C.-T. Ho and S. Sang, Essential Structural Requirements and Additive Effects for Flavonoids to Scavenge Methylglyoxal, *J. Agric. Food Chem.*, 2014, **62**, 3202–3210.

22 C. Crauste, M. Rosell, T. Durand and J. Vercauteren, Omega-3 polyunsaturated lipophenols, how and why?, *Biochimie*, 2016, **120**, 62–74.

23 C. Crauste, C. Vigor, P. Brabet, M. Picq, M. Lagarde, C. Hamel, T. Durand and J. Vercauteren, Synthesis and Evaluation of Polyunsaturated Fatty Acid-Phenol Conjugates as Anti-Carbonyl-Stress Lipophenols, *Eur. J. Org. Chem.*, 2014, 4548–4561.
24 E. Moine, M. Boukhallat, D. Cia, N. Jacquemot, L. Guillou, T. Durand, J. Vercauteren, P. Brabet and C. Crauste, New lipophenols prevent carbonyl and oxidative stresses involved in macular degeneration, *Free Radicals Biol. Med.*, 2021, **162**, 367–382.
25 A. Cubizolle, D. Cia, E. Moine, N. Jacquemot, L. Guillou, M. Rosell, C. Angebault-Prouteau, G. Lenaers, I. Meunier, J. Vercauteren, T. Durand, C. Crauste and P. Brabet, Isopropyl-phloroglucinol-DHA protects outer retinal cells against lethal dose of all-trans-retinal, *J. Cell. Mol. Med.*, 2020, **24**, 5057–5069.
26 N. Taveau, A. Cubizolle, L. Guillou, N. Pinquier, E. Moine, D. Cia, V. Kalatzis, J. Vercauteren, T. Durand, C. Crauste and P. Brabet, Preclinical pharmacology of a lipophenol in a mouse model of light-induced retinopathy, *Exp. Mol. Med.*, 2020, **52**, 1090–1101.
27 M. Vincent, L. Simon, P. Brabet, P. Legrand, C. Dorandeu, J. L. K. Him, T. Durand, C. Crauste and S. Begu, Formulation and Evaluation of SNEDDS Loaded with Original Lipophenol for the Oral Route to Prevent Dry AMD and Stragardt's Disease, *Pharmaceutics*, 2022, **14**, 1029.
28 W. Y. Oh, P. Ambigaipalan and F. Shahidi, Preparation of Quercetin Esters and Their Antioxidant Activity, *J. Agric. Food Chem.*, 2019, **67**, 10653–10659.
29 W. Y. Oh, P. Ambigaipalan and F. Shahidi, Quercetin and its ester derivatives inhibit oxidation of food, LDL and DNA, *Food Chem.*, 2021, **364**, 130394.
30 P. Torres, A. Poveda, J. Jimenez-Barbero, A. Ballesteros and F. J. Plou, Regioselective Lipase-Catalyzed Synthesis of 3-O-Acyl Derivatives of Resveratrol and Study of Their Antioxidant Properties, *J. Agric. Food Chem.*, 2010, **58**, 807–813.
31 L. Chebil, J. Anthoni, C. Humeau, C. Gerardin, J.-M. Engasser and M. Ghoul, Enzymatic Acylation of Flavonoids: Effect of the Nature of the Substrate, Origin of Lipase, and Operating Conditions on Conversion Yield and Regioselectivity, *J. Agric. Food Chem.*, 2007, **55**, 9496–9502.
32 A. Patti, M. Piattelli and G. Nicolosi, Use of Mucor miehei lipase in the preparation of long chain 3-O-acylcatechins, *J. Mol. Catal. B: Enzym.*, 2000, **10**, 577–582.
33 H. Peng and F. Shahidi, Quercetin Fatty Acid Monoesters (C2:0–C18:0): Enzymatic Preparation and Antioxidant Activity, *J. Agric. Food Chem.*, 2022, **70**, 14073–14083.
34 E. Moine, P. Brabet, L. Guillou, T. Durand, J. Vercauteren and C. Crauste, New Lipophenol Antioxidants Reduce Oxidative Damage in Retina Pigment Epithelial Cells, *Antioxidants*, 2018, **7**, 197.
35 M. Bouktaib, S. Lebrun, A. Atmani and C. Rolando, Hemisynthesis of all the O-monomethylated analogues of quercetin including the major metabolites, through selective protection of phenolic functions, *Tetrahedron*, 2002, **58**, 10001–10009.
36 M. Li, X. Han and B. Yu, Facile Synthesis of Flavonoid 7-O-Glycosides, *J. Org. Chem.*, 2003, **68**, 6842–6845.
37 J. Liu, J. Fu, W. Li, Y. Zou, Z. Huang, J. Xu, S. Peng and Y. Zhang, Utilization of the inherent nucleophile for regioselective O-acylation of polyphenols via an intermolecular cooperative transesterification, *Tetrahedron*, 2016, **72**, 4103–4110.
38 S.-H. Jung, H.-Y. Heo, J.-W. Choe, J. Kim and K. Lee, Anti-Melanogenic Properties of Velutin and Its Analogs, *Molecules*, 2021, **26**, 3033.